Journal of Materials Processing Technology 213 (2013) 1076–1087

Contents lists available at SciVerse ScienceDirect

Journal of Materials Processing Technology

journal homepage: www.elsevier.com/locate/jmatprotec

Carbon nanofiber assisted micro electro discharge machining of reaction-bonded silicon carbide

Pay Jun Liew[a,c], Jiwang Yan[b,*], Tsunemoto Kuriyagawa[a]

[a] Department of Mechanical Systems and Design, Tohoku University, Aramaki Aoba 6-6-01, Aoba-ku, Sendai 980-8579, Japan
[b] Department of Mechanical Engineering, Faculty of Science and Technology, Keio University, Hiyoshi 3-14-1, Kohoku-ku, Yokohama 223-8522, Japan
[c] Manufacturing Process Department, Faculty of Manufacturing Engineering, Universiti Teknikal Malaysia Melaka, Hang Tuah Jaya, 76100 Durian Tunggal, Melaka, Malaysia

ARTICLE INFO

Article history:
Received 4 July 2012
Received in revised form 26 January 2013
Accepted 3 February 2013
Available online 11 February 2013

Keywords:
Micro electro discharge machining
Carbon nanofiber
Reaction-bonded silicon carbide
Ultra-hard ceramics
Micro fabrication

ABSTRACT

Carbon nanofiber assisted micro electro discharge machining was proposed and experiments were performed on reaction-bonded silicon carbide. The changes in electro discharging behavior, material removal rate, electrode wear ratio, electrode geometry, spark gap, surface finish, surface topography and surface damage with carbon nanofiber concentration were examined. It has been found that the addition of carbon nanofiber not only improves the electro discharge frequency, material removal rate, discharge gap, but also reduces the electrode wear and electrode tip concavity. Bidirectional material migrations between the electrode and the workpiece surface were detected, and the migration behavior was strongly suppressed by carbon nanofiber addition. Adhesion of carbon nanofibers to the workpiece surface occurs, which contributes to the improvement of electro discharge machinability. These findings provide possibility for high-efficiency precision manufacturing of microstructures on ultra-hard ceramic materials.

1. Introduction

Micro machining of advanced engineering ceramics is currently gaining interests from multidisciplinary researchers. Reaction-bonded silicon carbide (RB-SiC) is one of the most promising engineering ceramics. It has excellent properties, such as high thermochemical stability, low density, high stiffness, high hardness, high thermal conductivity and low activation. RB-SiC is fabricated by infiltrating melted silicon into a green body consisting of carbon (C) and SiC powders, followed by reaction and sintering process at about 1700 K to form new SiC grains. In this way, a very dense material structure can be produced (Suyama et al., 2003).

Due to its high hardness, RB-SiC is extremely difficult to be machined. Many efforts have been made by previous researchers on abrasive machining of RB-SiC. For example, Tam et al. (2007) investigated the lapping and polishing of RB-SiC using various kinds of abrasives. Klocke and Zunke (2009) found that the material removal mechanisms of silicon based ceramics depend strongly on workpiece material properties, polishing agents as well as machining parameters. Generally speaking, abrasive machining processes produce a fine surface finish, but the material removal rate is low. Diamond cutting of RB-SiC was recently attempted by Yan et al. (2009), which could produce a high material removal rate. However, tool-wear still remains to be a problem in its industrial applications.

Electro discharge machining (EDM) is an alternative method to machine hard ceramics materials. A comparative study of the die-sinking EDM of three different ceramic materials was carried out by Puertas and Luis (2004). Clijsters et al. (2010) manufactured complex parts on SiSiC materials using EDM. However, most ceramics are not sufficiently conductive, which is a major problem when applying EDM to ceramics materials. Konig et al. (1998) indicated that the upper limit of electrical resistivity for a ceramic workpiece to be machined by EDM is 100 Ω cm. As pure SiC has a far higher electrical resistivity (~10^5 Ω cm), it is impossible to be machined directly by EDM. For RB-SiC, due to the presence of free Si (normally poly-crystalline) and other small-amount additives in the SiC bulk, the electrical conductivity can be improved to some extent (Wilhelm et al., 1999). Even though, the conductivity of RB-SiC is still very poor if compared to other conductive materials. Hence, the EDM machining efficiency of RB-SiC is extremely low and the EDM process is unstable.

In order to improve the EDM machinability of materials, a number of researchers attempted adding conductive powders into dielectric fluids. For example, Yeo et al. (2007) added 45–55 nm-sized SiC powders into dielectric and found that the surface craters became smaller than those produced in powder free dielectric fluid. Chow et al. (2008) added SiC powders into pure water as dielectric fluid in the EDM of titanium alloy, and confirmed the improvement in surface quality and material removal rate. Gunawan et al. (2009)

* Corresponding author. Tel.: +81 45 566 1445; fax: +81 45 566 1495.
E-mail address: yan@mech.keio.ac.jp (J. Yan).

0924-0136/$ – see front matter © 2013 Elsevier B.V. All rights reserved.
http://dx.doi.org/10.1016/j.jmatprotec.2013.02.004

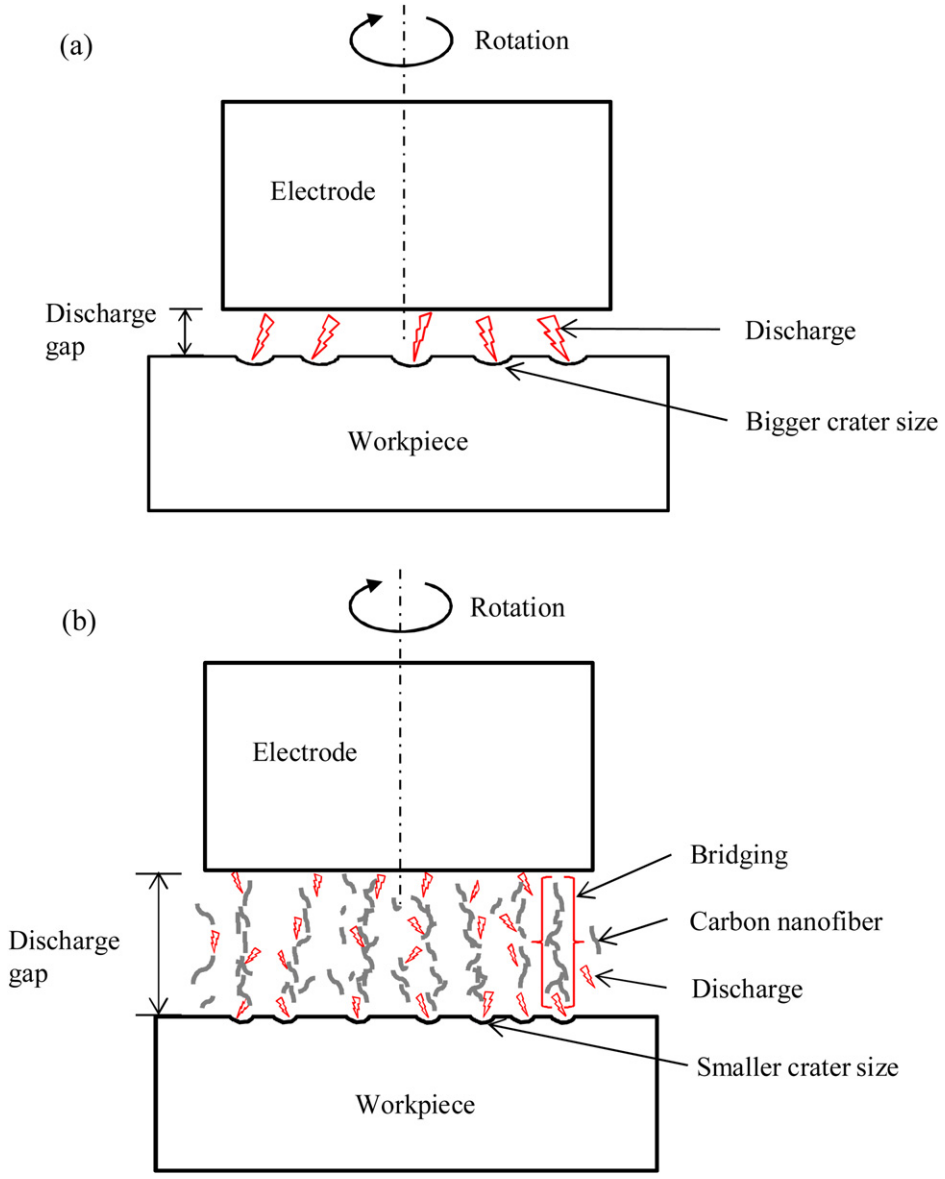

Fig. 1. Schematic model for (a) conventional EDM and (b) carbon nanofiber assisted micro EDM.

added molybdenum disulfide (MoS_2) powders and improved the material removal rate and surface roughness of Cu, brass and Cu–W workpiece materials. Gunawan et al. (2011) also tried suspending nano graphite powder in dielectric fluid with the combination of ultrasonic vibration. They found that the machining time was reduced up to 35%. Powder assisted EDM was also applied to the EDM of ceramic materials. Jahan et al. (2010a, b) studied the effect of adding graphite, aluminum and non-conductive alumina powders in EDM of tungsten carbide ceramics. They found that the graphite powder provided a smooth surface and the aluminum powder resulted in higher spark gap and higher material removal rate, whereas the alumina powder had little effect on the EDM performance. Nevertheless, for low-conductivity or insulating ceramic materials, it was difficult to obtain good machining performance by powder addition. For example, Tani et al. (2002) used Al, Gr, Si, Ni, ZrB_2 powders to assist the EDM of insulating Si_3N_4 ceramics and found that even though the removal rate was increased, the surface roughness was barely improved. This was due to the generation of long pulse discharge in the EDM process.

In this study, carbon nanofibers assisted micro EDM of RB-SiC is proposed. As schematically shown in Fig. 1, unlike the conventional EDM and powder assisted EDM, carbon nanofibers can arrange themselves in the form of micro chains by interlocking which helps to form bridging networks between electrode and workpiece. The excellent electrical conductivity of carbon nanofiber also reduces the insulating strength of the dielectric fluid and increases the spark gap distance between the electrode and workpiece. As a result, the frequency of electro discharge and the material removal rate in the EDM of RB-SiC might be improved. In addition, multiple fine discharges might occur under this situation, leading to a reduction in crater size on the workpiece surface, and in turn, a better surface finish might be obtained. In this work, the effect of carbon nanofiber addition on the electro discharge behavior, material removal rate, electrode wear rate, electrode geometry, spark gap,

Table 1
Properties of workpiece material (RB-SiC).

Properties	Values
Si/SiC volume ratio (%/%)	12/88
Density ρ (g/cm^3)	3.12
Softening temperature (°C)	1375
Young modulus E (GPa)	407
Bending strength R_T (MPa)	780
Thermal expansion coefficient (10^{-6} K^{-1})	3.23
Thermal conductivity (W/m K)	143
Porosity (%)	<0.1

workpiece surface roughness, surface topography and surface damage were investigated experimentally.

2. Experimental methods

2.1. Machine tool

A micro EDM machine, Panasonic MG-ED82W, was used in the experiments. This EDM machine has a resistor–capacitor (RC) circuit for electro-discharge. The electrical capacitance is determined by condensers C1–C4, the capacities of which are 3300 pF, 220 pF, 100 pF and 10 pF, respectively. The machine enables both micro wire EDM and micro die sinking machining. The maximum travel ranges of the machine tables are 200 mm in X direction, 50 mm in Y direction, and 50 mm in Z direction, with a stepping resolution of 0.1 μm.

2.2. Electrode

Tungsten rods with 300 μm diameters were used as tool electrodes. Before the EDM of RB-SiC, the tool electrode tips were dressed by using wire electro discharge grinding (WEDG) in order to improve their form accuracy. Electrode dressing was also performed after each EDM cycle because the tip electrode, especially the corner, will wear. In the WEDG, a brass wire (diameter 100 μm) with positive electrode polarity was used to machine the tool electrode which was rotated at a rotation speed of 3000 rpm by the machine spindle. Using the WEDG fabricated electrodes, machining tests of micro cavities were performed on RB-SiC using die sinking EDM, where negative electrode polarity was used.

2.3. Workpiece

The workpiece material used in the experiments was RB-SiC (Japan Fine Ceramics Co., Ltd.). The as-received samples were cylinders with a diameter of 30 mm and a thickness of 10 mm. The volume ratio of residual Si bond is 12%, and the average size of the 6H–SiC grains is less than 1 μm. Some typical material properties of the sample are shown in Table 1.

The electrical resistivity of the sample is 1453 Ω cm. To compare the EDM machinability, a few preliminary EDM tests were performed on the RB-SiC workpiece and stainless steel SUS304. Fig. 2 shows measurement results of electrical currents in the EDM of SUS304 and RB-SiC, respectively. The experiment was performed using a tungsten electrode with a diameter of 47 μm at a voltage of 80 V and a condenser of 100 pF that is suggested by the micro EDM machine manufacturer, and the electrical current measurement was performed using Tektronix TDS2024B with current probe CT-2. It is clear that for SUS304, the pulse is very sharp with a pulse width of 25 ns and a peak electrical current of 0.9 A. In contrast, for RB-SiC the pulse width is 220 ns and the peak electrical current is only 0.1 A. This distinct difference in electrical current pulse shape indicates that the EDM machinability of RB-SiC is far lower than the stainless steel.

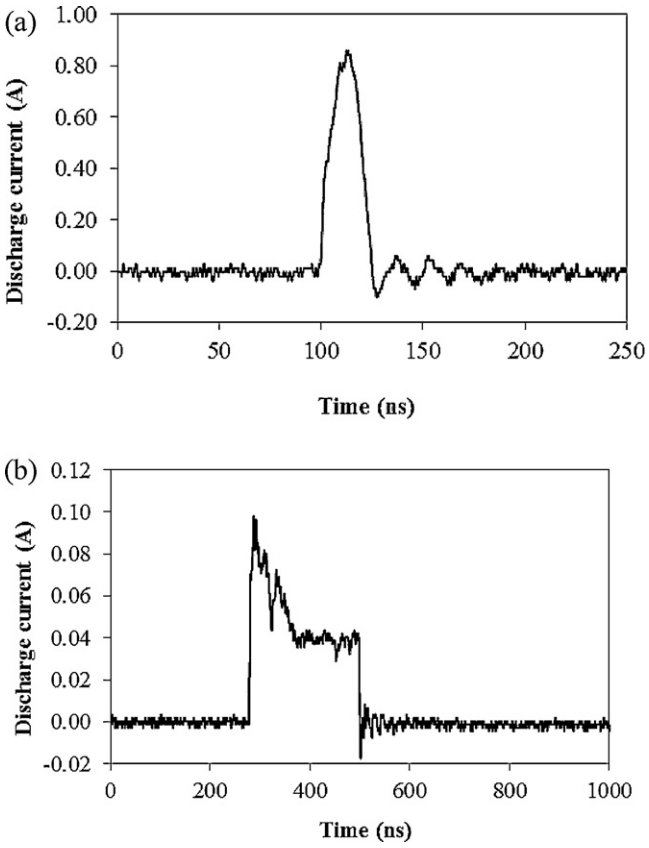

Fig. 2. Electrical current waveforms in EDM of (a) SUS304 and (b) RB-SiC.

2.4. Carbon nanofiber

Carbon nanofibers used in this study are 150 nm in diameter and 6–8 μm in length. Fig. 3 shows a scanning electron microscope (SEM) micrograph of the carbon nanofibers. Different fiber concentrations ranging from 0 to 0.28 g/L were used. The dielectric fluid used was hydrocarbon dielectric oil CASTY-LUBE EDS, which has a high flash point. In order to prepare the mixed dielectric, the required amounts of carbon nanofibers and dielectric fluid were measured separately before being mixed together and homogenized in a mixer for 20 min. This is to ensure that the carbon nanofibers are uniformly dispersed in the dielectric fluid.

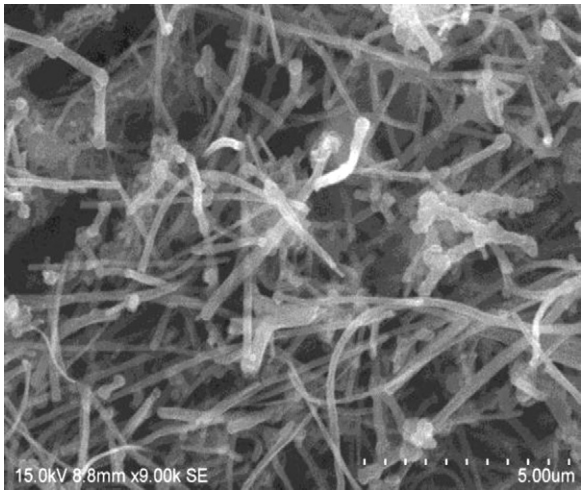

Fig. 3. SEM micrograph of carbon nanofibers.

Table 2
Experimental conditions.

Workpiece material	RB-SiC
Electrode material	Tungsten
Polarity	Positive (workpiece) Negative (tool electrode)
Rotational speed	3000 rpm
Voltage	110 V
Condenser capacitance	3300 pF
Feed rate	3 μm/s
Dielectric fluid	EDM oil CASTY-LUBE EDS
Additive	Carbon nanofibers
Concentration	0–0.28 g/L
Machining time	5 min
Cavity depth	20 μm

2.5. Machining conditions

Table 2 shows the experimental conditions. For comparison, two types of EDM tests were carried out under different fiber concentrations: (1) time-controlling method, where each trial run was performed for duration of 5 min, and (2) depth-controlling method, where die sinking micro EDM tests were performed until a depth of 20 μm. Normally, depth-controlling method is used for rough machining (shape generating) and time-controlling method is used for fine machining (surface finishing).

2.6. Measurement and evaluation

Surface roughness of the workpiece and cross-sectional profile of electrode tip after the EDM tests were measured using a laser probe profilometer NH-3SP (Mitaka Kouki Co. Ltd.). The measurement of surface roughness was performed across the center of the micro cavity along the radial direction, and the evaluation length was 100 μm. The machined surface of the micro cavities were then examined using a scanning electron microscope (SEM) and energy dispersive X-ray (EDX). An optical microscope was used to measure the dimension of the electrode and the size of the cavity after each experiment.

3. Results and discussion

3.1. Electro discharge behavior

To directly examine the effect of carbon nanofiber addition on electro discharge behavior, a high speed camera system was used to observe the EDM region. Fig. 4 shows high speed camera images of spark generation during micro EDM without carbon nanofiber addition and with carbon nanofiber addition (concentration 0.06 g/L), respectively. It is clear that the spark region in Fig. 4(b) is distinctly bigger than that of (a), indicating that electro discharge has been significantly activated by carbon nanofiber addition. Next, the discharge voltage waveforms were observed using an oscilloscope Texio DCS 9515. Fig. 5 shows the voltage waveforms for micro EDM without carbon nanofiber addition and with carbon nanofiber addition (concentration 0.06 g/L), respectively. During the same period of time (1000 μs), the pulse number of discharge voltage in Fig. 5(b) is 37, while that in Fig. 5(a) is only 2. This result demonstrates again that due to the carbon nanofiber addition, the electro discharge characteristics in EDM of RB-SiC have been greatly improved. It should be noted that in Fig. 5(b), a multiple discharging effect (several discharging paths are generated within one single input pulse) was observed within a single input pulse, indicating that the discharging energy has been dispersed by the fiber addition.

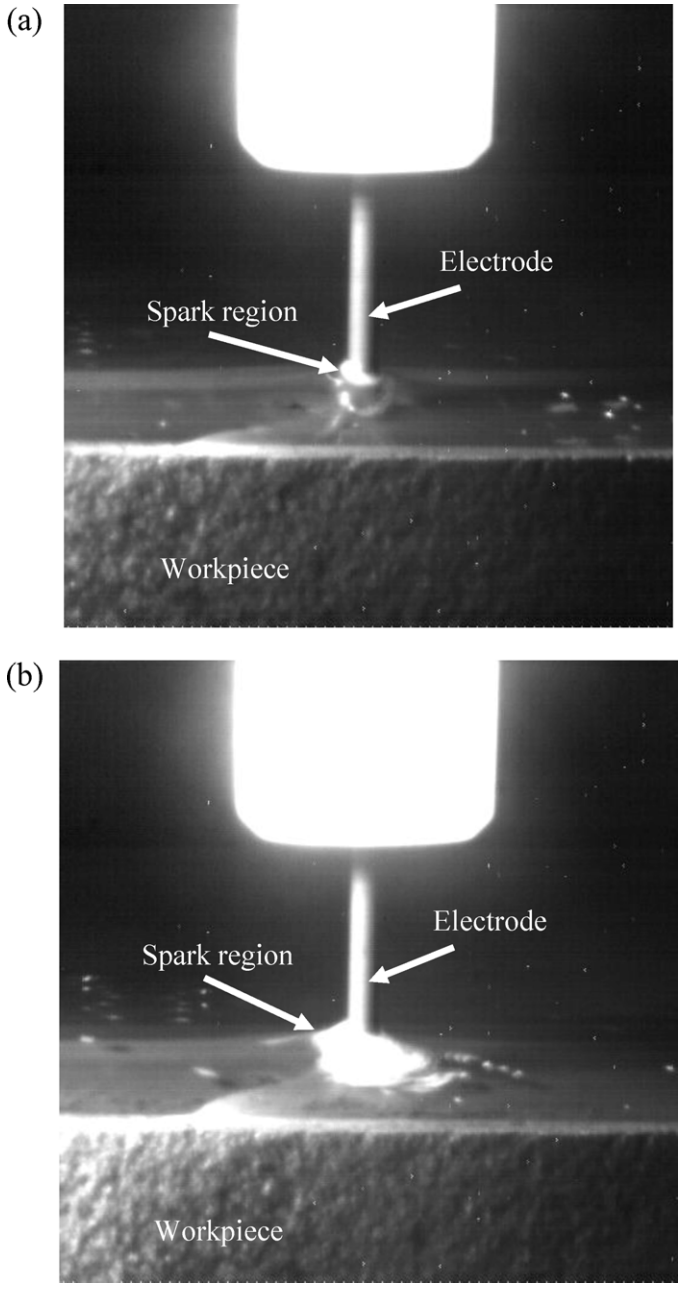

Fig. 4. High speed camera observation of spark generation during micro EDM: (a) without and (b) with carbon nanofiber addition.

3.2. Material removal rate

Material removal rate (MRR) was calculated as the volume of material removed from workpiece over a period of time. The laser probe profilometer NH-3SP was used to scan across the machined area, as shown in Fig. 6, and the volume of material removed was obtained by analyzing the three-dimensional surface topography.

Fig. 7 shows the effect of concentration of carbon nanofiber on the MRR of RB-SiC. When no carbon nanofibers were added into the dielectric fluid, the MRR is extremely low. However, the MRR increases rapidly with the increase of the concentration of carbon nanofibers, and the maximum MRR is found at the concentration of 0.17 g/L for both time-controlling and depth-controlling conditions. This result agrees with the observation results in Section 3.1, and demonstrates again that the frequency

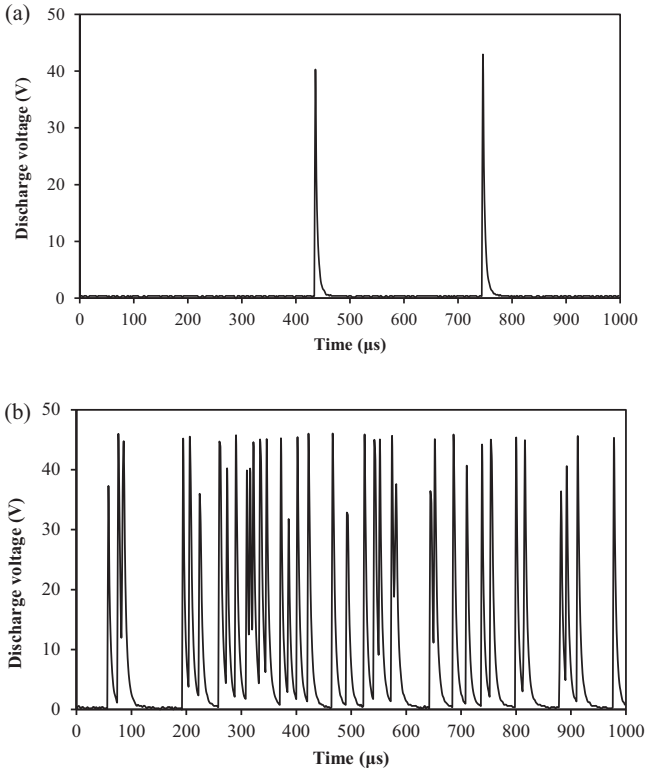

Fig. 5. Discharge voltage waveform during micro EDM: (a) without and (b) with carbon nanofiber addition.

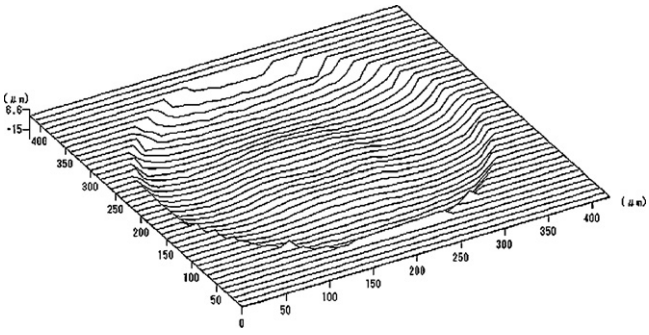

Fig. 6. Three-dimensional topography of a machined cavity for the measurement of volume of material removed from workpiece.

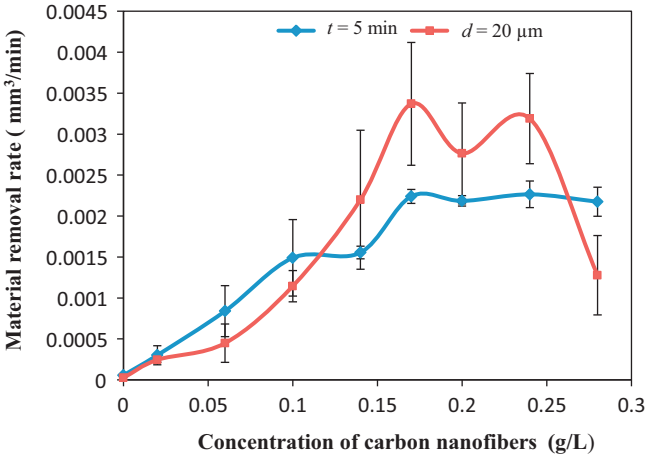

Fig. 7. Effect of carbon nanofibers concentration on material removal rate.

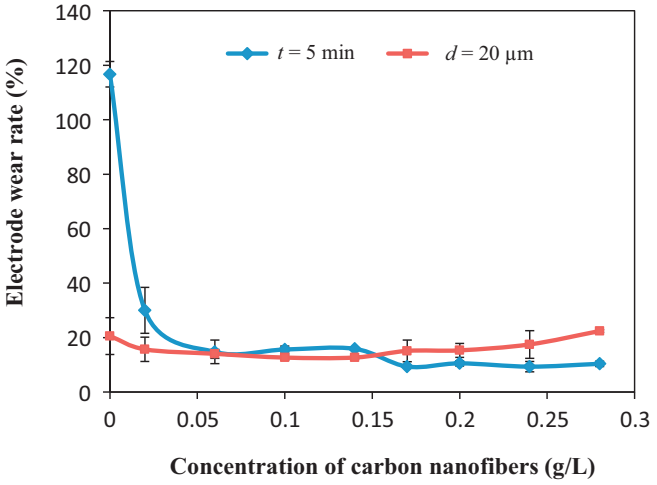

Fig. 8. Effect of carbon nanofibers concentration on electrode wear rate.

of discharge will be increased and the EDM machinability has been improved by adding carbon nanofibers into the dielectric fluid.

It should be noted that there is an optimum range for carbon nanofiber concentration. In Fig. 7, for fiber concentrations higher than 0.17 g/L, the MRR tends to reduce (for the depth controlling machining) or keep almost constant (for the time-controlling machining). This trend is consistent with that reported by Jahan et al. (2010a). At an excessively high concentration of powder (in this case, carbon nanofibers) additive, the deposited powders cannot be removed easily from the machining gap and caused the secondary sparking. This secondary sparking makes the machining unstable and increases the machining time, leading to the reduction of MRR.

3.3. Electrode wear ratio

Electrode wear ratio (EWR) is defined as the ratio of volume of material removed from electrode to the volume of material removed from the workpiece at the same time span. The change of EWR versus carbon nanofiber concentration is depicted in Fig. 8. Under the time-controlling condition, the EWR dropped significantly when the carbon nanofibers were added, and then keep constant when further increasing the concentration of the carbon nanofibers. As known from Paramjit et al. (2010), EWR is high when using pure dielectric fluid because of that the ions produced by the ionization of dielectric fluid hit the tool electrode with high momentum and high energy, which causes rapid erosion of the tool electrode. The addition of carbon nanofibers into the dielectric fluid might have prevented the ionization phenomenon.

It is noticed that under the depth-controlling condition, the change of EWR was not so significant. This might be because of that the machining time for a constant depth of 20 μm was shorter if compared to time-controlling condition (5 min) when carbon nanofibers were added. In this case, more materials were removed from the workpiece than from the electrode. However, when no carbon nanofibers were added, even though a longer machining time was taken, short circuit and tool electrode back feeding occurred frequently, causing decrease in the frequency of discharge and resulting lower erosion of tool electrode. Thus, there is no significant different of EWR with and without carbon nanofibers addition under the depth-controlling condition.

Next, tool electrode geometry after EDM was investigated. Fig. 9 presents SEM micrographs of tungsten electrode tip after micro EDM experiments under depth controlling condition. The

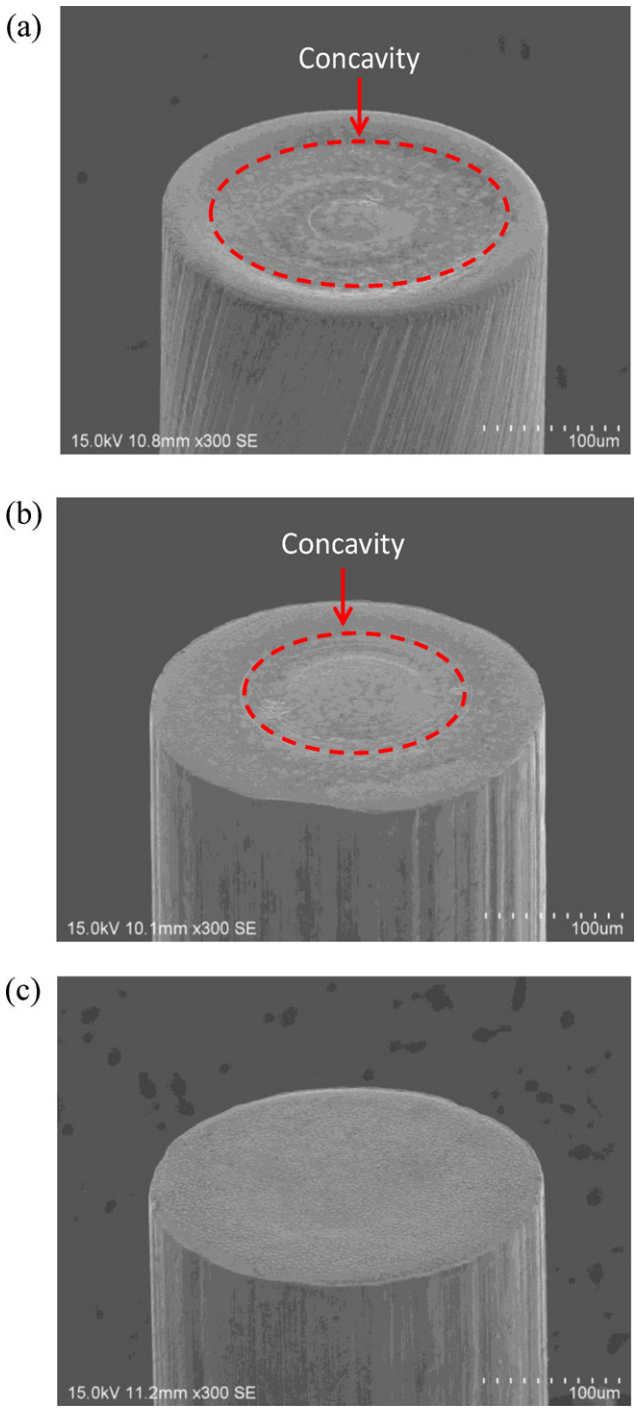

Fig. 9. SEM micrograph of tungsten electrode tip at machining depth of 20 μm: (a) without and (b) with 0.02 g/L and (c) 0.10 g/L carbon nanofibers.

cross-sectional profile of electrode tip measured by laser probe profilometer NH-3SP is shown in Fig. 10. Besides the corner wear and end wear, hole wear occurred in the center of tungsten tip, forming a concave shape (Fig. 9(a)). Interestingly, the concave shape became insignificant, i.e., the electrode tip became flat, when carbon nanofibers were added in the dielectric fluid (Fig. 9(c)). In the sparking gap, the stagnation of debris occurs intensively in the center of the micro cavity, where the debris particles interact with the tool electrode (Ekmekci and Sayar, 2013), causing the concavities in the center of tool tip. Without the addition of carbon nanofibers, the piled debris density is typically higher than the one with carbon nanofibers addition, causing bigger concavity on

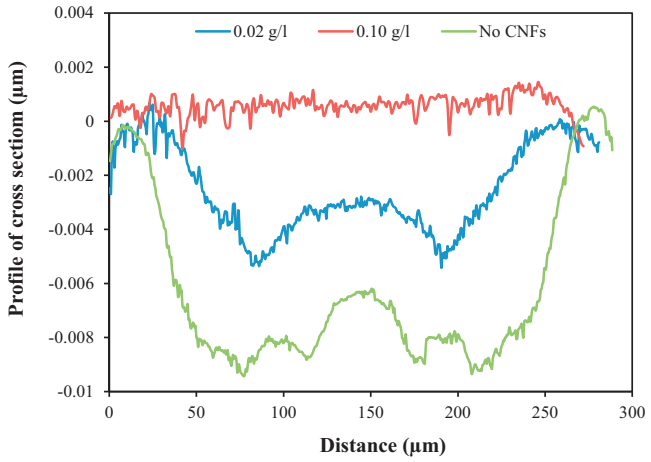

Fig. 10. Comparison of cross sectional profiles of tungsten electrode tip after micro EDM under depth controlling condition.

the tool tip. Increasing carbon nanofibers concentration is helpful for preventing the concavity formation, where effective flushing takes place due to the bigger sparking gap, and in turn, better form accuracy can be obtained.

3.4. Spark gap

Spark gap was obtained by measuring the diameters of the micro cavities and the electrodes after each machining test. The diameters of micro cavities obtained under time-controlling and depth-controlling conditions ranged from 332 μm to 350 μm, and from 337 μm to 353 μm, respectively. Fig. 11 illustrates the effect of carbon nanofiber concentration on spark gap. It is seen that the spark gap increases with the increase of fiber concentration. The addition of carbon nanofiber improves the breakdown strength of dielectric and causes the insulating strength of dielectric fluid to reduce (Tzeng and Chen, 2005). As a result, a bigger spark gap will be maintained, and the debris will be flushed out more easily if compare to the results under pure dielectric fluid.

When no carbon nanofibers were added, the discharge gap between the electrode and workpiece is extremely small, so that the debris could not be removed effectively from the gap, thus short circuit takes place between the electrode and workpiece. When short circuit occurs, the electrode will immediately move in the reverse

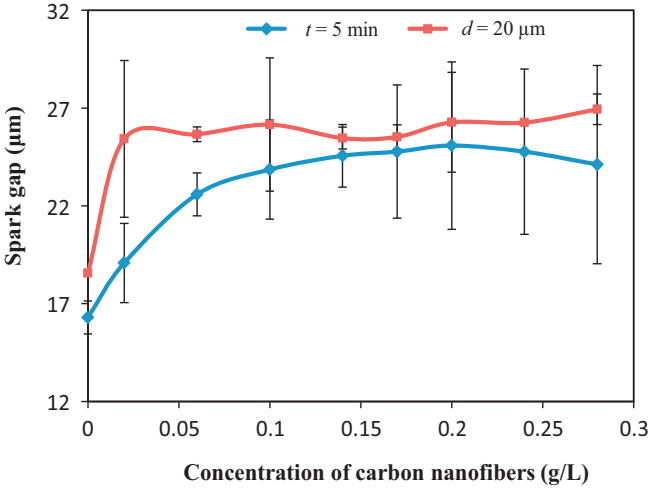

Fig. 11. Effect of carbon nanofibers concentration on spark gap.

direction of the feed to maintain a bigger gap (Takashi et al., 2008). The back feeding action will cause a low MRR. When the carbon nanofibers were added into the dielectric fluid, however, the insulating strength of dielectric fluid will be reduced, which results in a bigger discharge gap between the tool electrode and the workpiece. In this case, debris will be effectively removed from the gap and short circuit will be prevented.

3.5. Surface roughness

The effect of carbon nanofiber concentration on the surface roughness of the machined surface is shown in Fig. 12. Under the time-controlling condition, the surface roughness tends to decrease sharply at a fiber concentration of 0.02 g/L, and then increases gradually as fiber concentration increases further. Under the depth-controlling conditions, the surface roughness decreases with fiber concentration until 0.1 g/L, and as fiber concentration increases further, the surface roughness tends to increase again.

As demonstrated by Paramjit et al. (2010), adding a suitable amount of powders will lead to uniform dispersion of discharge energy in all directions and cause a decrease in crater size, thus surface finish will be improved. At a very high concentration of powder additive, however, the dielectric might lose its ability to distribute uniformly the powder materials. Therefore, the carbon nanofibers may accumulate together, bridging the discharge gap and resulting in arcing and short circuiting more frequently. This effect will finally increase the surface roughness (Jahan et al., 2010a). In the present experiments, the optimum carbon nanofiber concentration is around 0.02 g/L under the time-controlling conditions, and 0.06–0.1 g/L under the depth-controlling conditions.

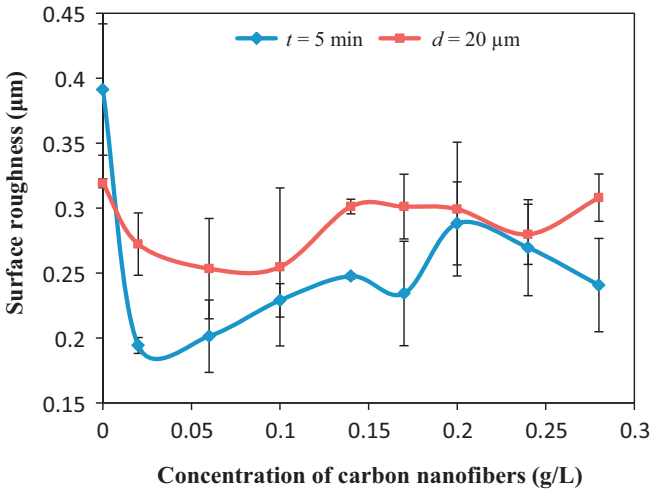

Fig. 12. Effect of carbon nanofibers concentration on surface roughness.

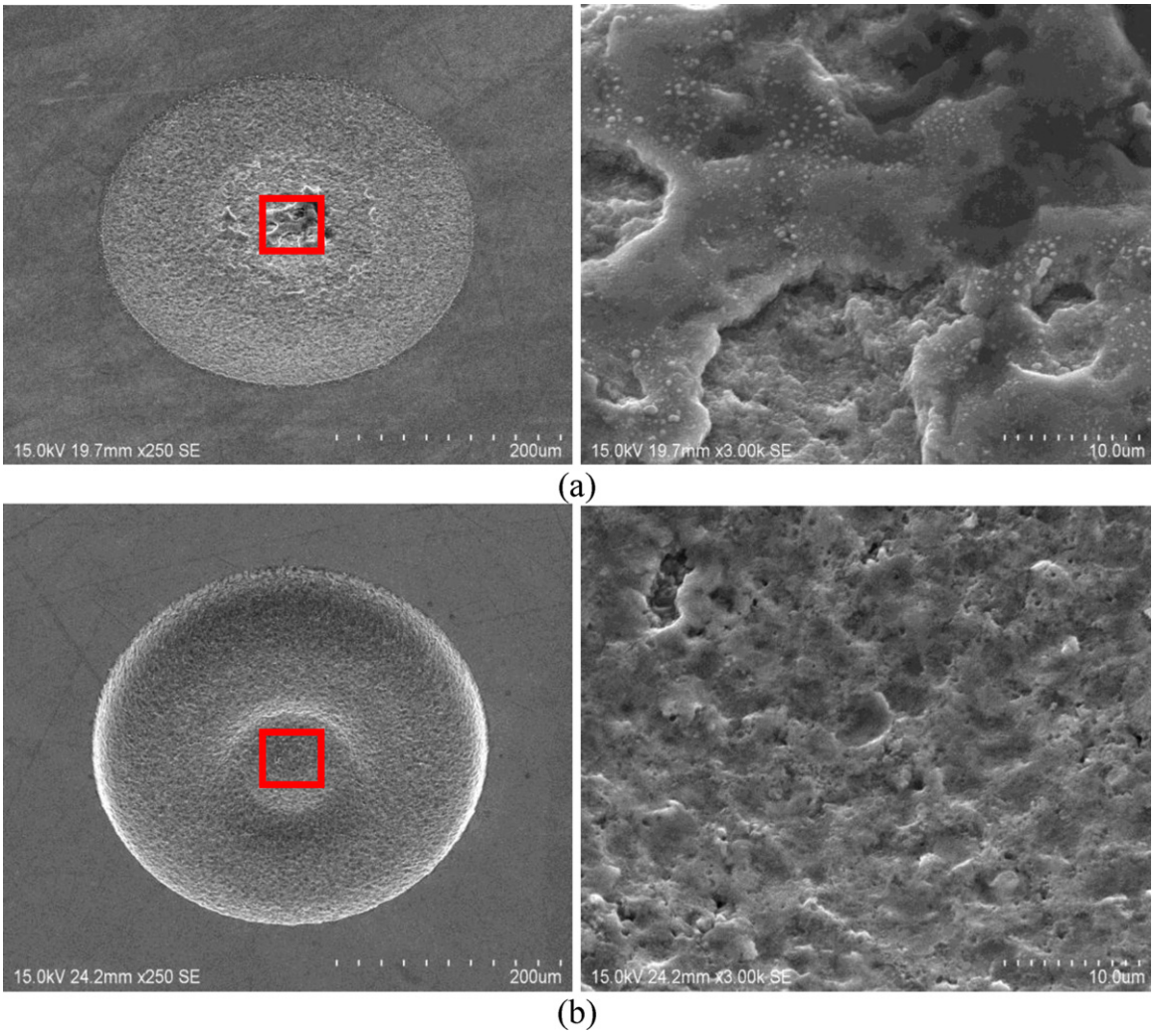

Fig. 13. Comparison of machined surface after machining time of 5 min: (a) without and (b) with 0.06 g/L carbon nanofibers.

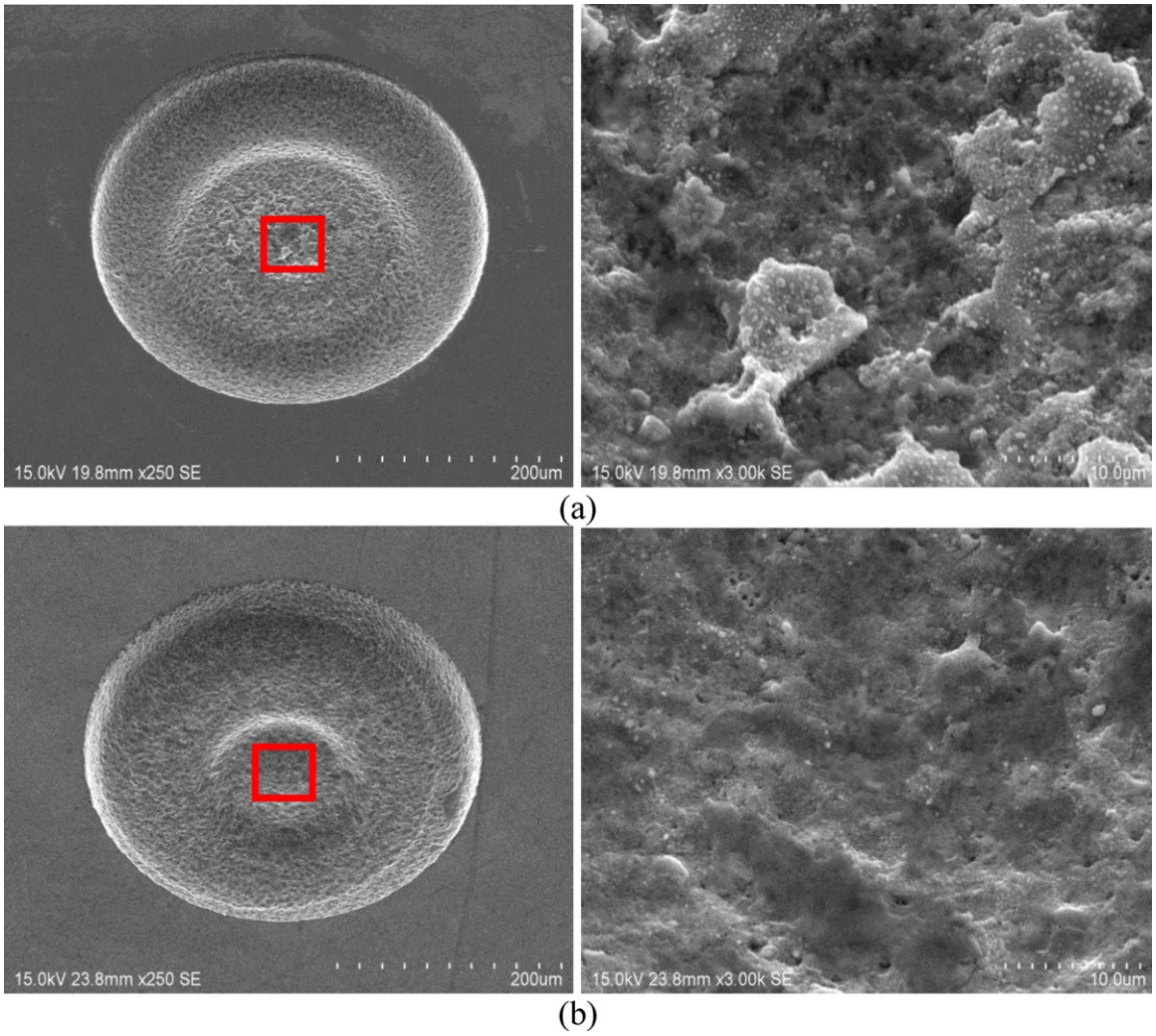

Fig. 14. Comparison of machined surface at machining depth of 20 μm: (a) without and (b) with 0.06 g/L carbon nanofibers.

3.6. Surface topography

Fig. 13 shows SEM micrographs of the machined micro cavities obtained with and without carbon nanofiber addition, respectively, under the time-controlling conditions. The left micrographs are low-magnification views and the right ones are high-magnification views of the center regions of the left ones. It is clear that the machined surface with carbon nanofibers additive (Fig. 13(b)) is smoother compared to the one obtained with pure dielectric fluid (Fig. 13(a)). Without the carbon nanofibers additive, the materials of RB-SiC were removed as large flakes, leading to very large craters (10 μm level); while with carbon nanofiber addition, the surface craters are extremely small (μm level). For comparison, SEM micrographs of the machined micro cavities under the depth-controlling conditions are shown in Fig. 14. Similarly, the machined surface with fiber additive is apparently smoother (Fig. 14(b)) if compared to the one obtained with pure dielectric fluid (Fig. 14(a)).

As mentioned in Section 3.4, with carbon nanofiber additive in the dielectric fluid, the sparking gap has been increased; consequently the debris causing secondary discharge can be flushed out from the gap more easily. The adhesion of resolidified debris on the machined surface is reduced, which results a better surface topography. Furthermore, the discharge distribution becomes more uniform, hence uniformly small craters were produced on the machined surface (Jahan et al., 2010b). If no carbon nanofibers were used, however, the discharging process is unstable, and material is removed through spalling, in which surface layers of the workpiece material are fractured as large flakes by thermal shocks. This is distinctly different from normal spark erosion which involves melting, dissociation and evaporation of material (Trueman and Huddleston, 2000). This result strongly demonstrates that adding carbon nanofibers in the dielectric fluid is helpful for improving the surface finish of RB-SiC.

In addition, it can be seen from Figs. 13 and 14 that cone-shape protrusions were formed in the center of the micro cavities. This is presumably because of the debris were not drawn out from the center region and second electric discharges occurred. However, the cone-shape protrusions when carbon nanofibers were mixed in the dielectric fluid were smaller than those when pure dielectric fluid was used. The sparking gap in the carbon nanofibers mixed dielectric fluid is bigger, so the stagnation of debris in the center of the micro cavity is reduced. These results are symmetry with the concavity that was formed in the center of the electrode tip, as explained in Section 3.3.

Subsequently, surface damage in micro cavity after micro EDM was investigated. Fig. 15 presents SEM micrographs of surfaces of micro cavities obtained with and without carbon nanofiber addition, respectively, under the time-controlling conditions. It can be seen that for both conditions, the machined surface covered with micro defects such as micropores and microcrack, regardless of the

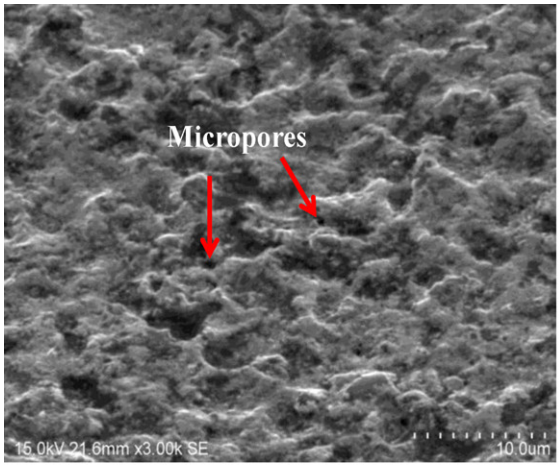

(a)

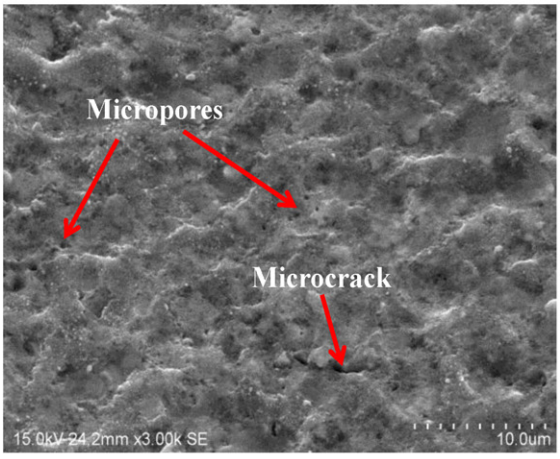

(b)

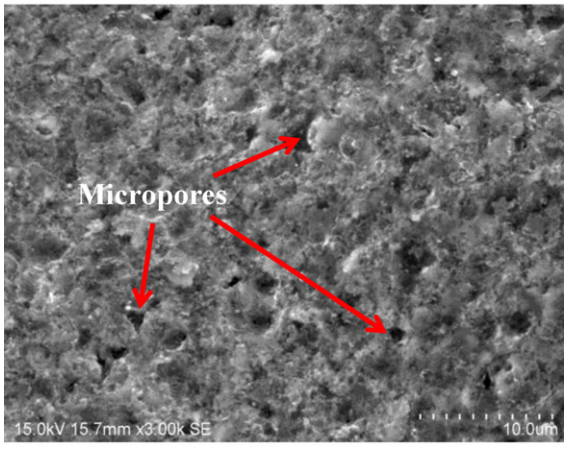

(c)

Fig. 15. SEM micrograph of machined surface, showing the existence of microcracks and micropores after machining time of 5 min: (a) without and (b) with 0.02 g/L and (c) 0.14 g/L carbon nanofibers.

craters produced with pure dielectric fluid (Fig. 15(a)). Moreover, it is noteworthy that by using higher carbon nanofiber concentration, such as 0.14 g/L as demonstrated in Fig. 15(c), the size and density of the micropores are bigger compared to the one obtained with lower carbon nanofiber concentration, 0.02 g/L as shown in Fig. 15(b). Similar trend was confirmed in the results obtained under the depth-controlling conditions.

According to Lee et al. (1988) and Lauwers et al. (2004), the formation of micropores is associated with the ejection of entrapped gas from the redeposited material, and the microcracks are formed as a result of the high contraction stress that exceeds the ultimate strength of the specimen surface (Ekmekci et al., 2009; Lee et al., 1988). However, careful examinations on the microstructure that produced by higher carbon nanofiber concentration (Fig. 15(c)) revealed that micropore size is about 5–8 times bigger than the one obtained with lower carbon nanofiber concentrations. This phenomenon indicates that the mechanism of micropore formation on RB-SiC ceramic at high carbon nanofiber concentration maybe different from that of the micro EDM of conductive metals. That is, besides the ejection of gases, the preferential removal of Si binder from the workpiece surface may lead to the formation of micropores. Since the Si matrix, in conjunction with sintering agents, possesses a higher electrical conductivity than the SiC grains, it will be preferentially removed by melting and vaporization (Konig et al., 1998) induced by higher discharge density at high carbon nanofibers concentration. This effect will leave micropores on the machined surface, and in turn, increase the surface roughness. Therefore, optimizing the amount of carbon nanofiber is important for improving surface roughness and preventing surface damage.

3.7. Material migration phenomena

Fig. 16 shows SEM micrograph and an EDX spectrum of a micro cavity machined by micro EDM with carbon nanofiber addition. For comparison, the results for micro EDM without fiber addition are shown in Fig. 17. In Figs. 16(b) and 17(b), it can be seen that besides the parent materials of RB-SiC, such as C and Si (O is presumably from the atmosphere), the electrode material tungsten (W) has been detected on the machined workpiece surface. This result indicates that there is a migration of material from the electrode to the machined surface, as reported by Soni and Chakraverti (1996). In addition, comparing Figs. 16(b) and 17(b), it is noteworthy that the tungsten material transfer from the electrode to the workpiece in pure dielectric fluid is higher than the one obtained in carbon nanofiber mixed fluid. This fact demonstrated that adding carbon nanofibers in dielectric fluid at a suitable concentration is helpful for preventing material migration, and in turn, reduces tool electrode wear.

Fig. 18(a) shows SEM micrograph of a tungsten electrode tip after micro EDM, and Fig. 18(b) shows its EDX spectrum analysis results. The element C has been detected on the electrode tip as indicated in Fig. 18(a), indicating that during EDM the carbon element from the nanofibers, dielectric oil or the workpiece material has also been partially transferred to the electrode surface. From this fact, one can say that the material migration between tool electrode and workpiece is a bidirectional phenomenon. In addition, since Si element was not found on the tool surface, it is presumable that material migration from the workpiece to the electrode is insignificant compared to that from carbon nanofibers or dielectric oil to electrode.

Fig. 19 presents high magnification SEM micrographs (left: 10 000×; right: 50 000×) of machined RB-SiC surface at carbon nanofiber concentrations of 0.14 g/L and 0.24 g/L, respectively. It was found that a few carbon nanofibers have been deposited onto the workpiece surface after the EDM process. Similarly, Ekmekci and Ersoz (2012) also reported that cubic shaped SiC particles partly penetrated into the substrate material by means of electrophoresis and negative pressure induced after cessation of a discharge when water dielectric liquid was used. Empirically, the higher the carbon nanofiber concentration is, the

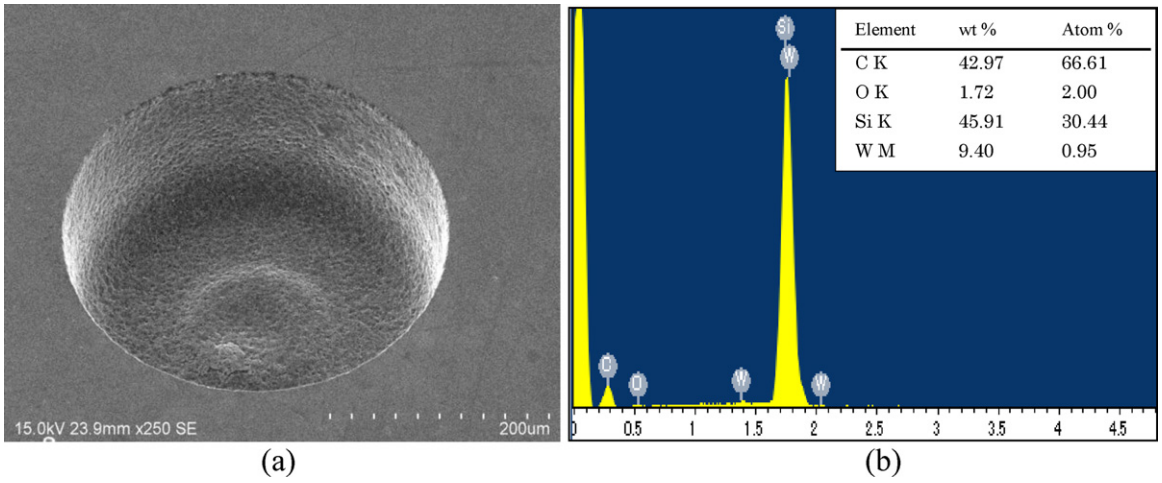

Fig. 16. (a) SEM micrograph and (b) EDX spectrum analysis of a machined cavity at carbon nanofiber concentration of 0.28 g/L.

more fibers are deposited. The fiber adhesion to the workpiece was so strong that they could not be removed even the workpiece was washed in acetone using an ultrasonic cleaner. The adhered carbon nanofibers may significantly improve the electrical conductivity of the workpiece surface, which might help to improve the EDM machinability of this material. The material migration phenomenon will be further investigated in our future work.

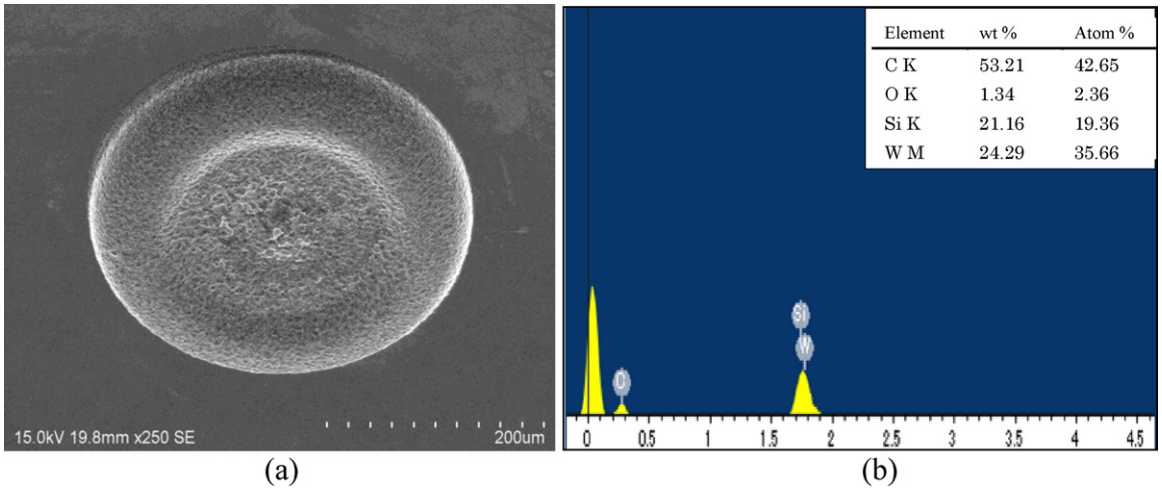

Fig. 17. (a) SEM micrograph and (b) EDX spectrum analysis of a machined cavity without carbon nanofiber.

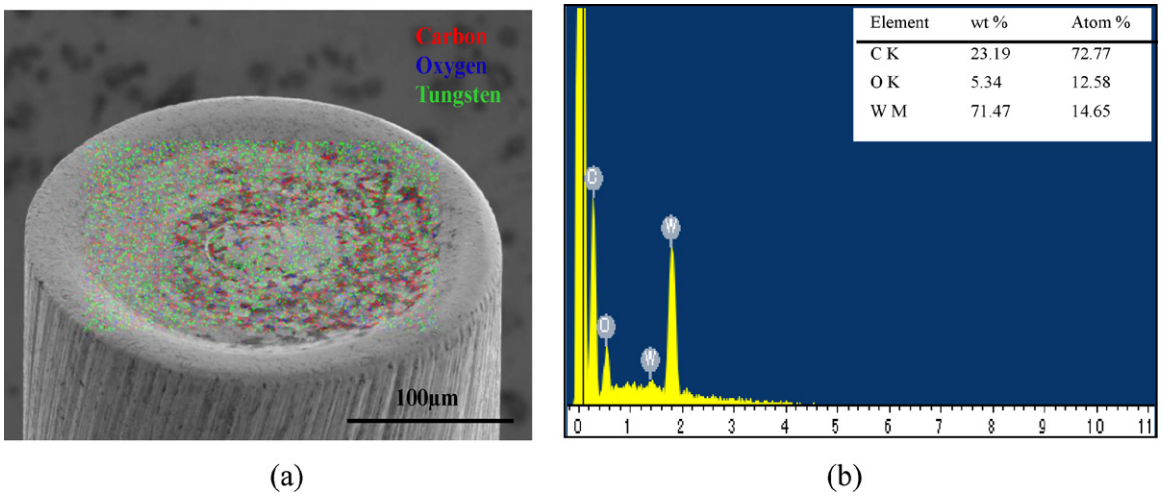

Fig. 18. (a) SEM micrograph and (b) EDX spectrum analysis of a tungsten electrode tip after micro EDM.

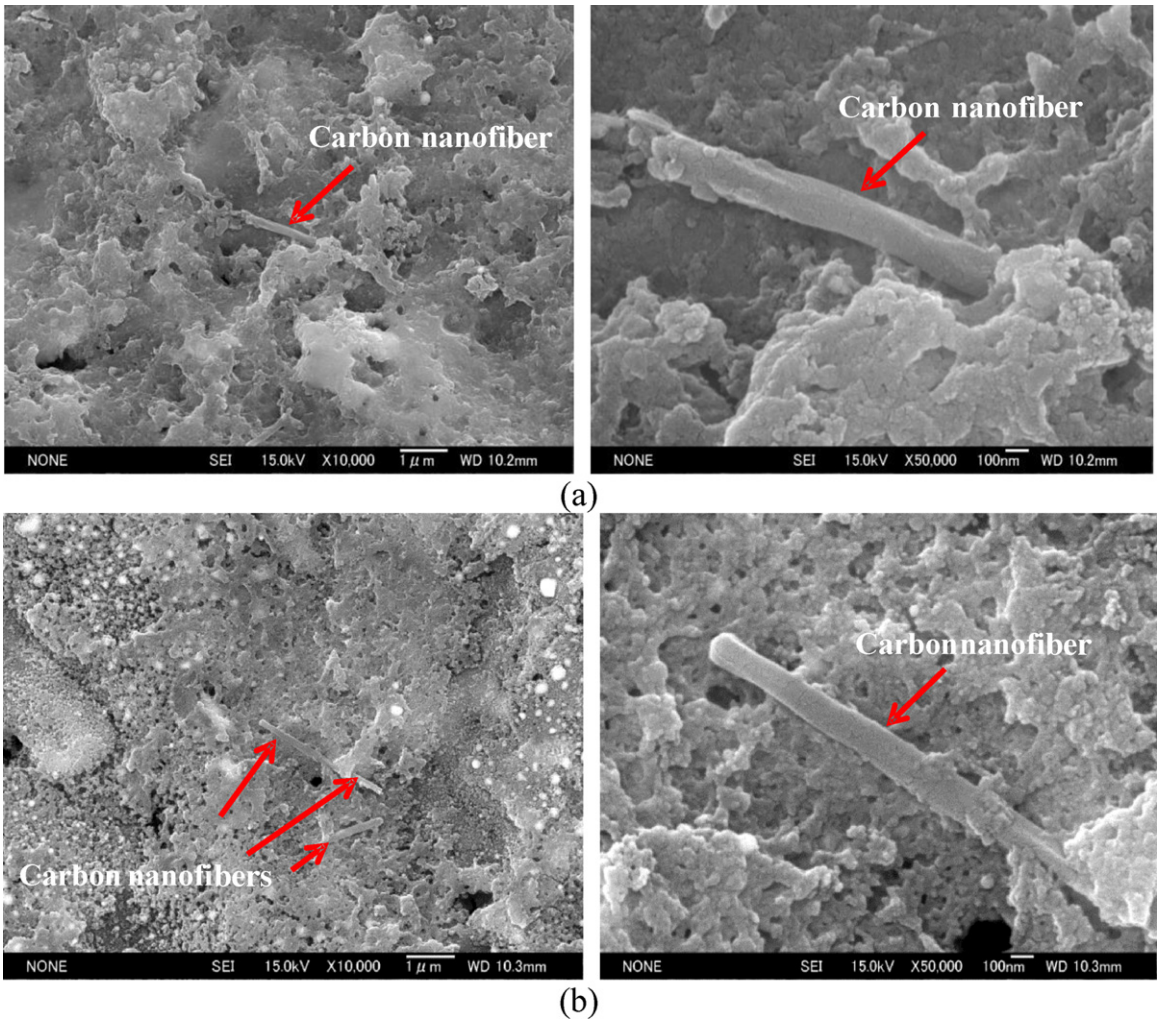

Fig. 19. SEM micrographs of machined surfaces after machining for 5 min at different carbon nanofibers concentrations: (a) 0.14 g/L and (b) 0.24 g/L.

4. Conclusions

Carbon nanofiber assisted micro EDM of RB-SiC was proposed. The effect of carbon nanofiber addition on the electro discharge behavior, material removal rate, electrode wear ratio, electrode geometry, spark gap, surface roughness, surface topography, and surface damage was investigated. The major conclusions are summarized as follows:

1. Adding carbon nanofibers into the dielectric fluid can significantly improve the electro discharge frequency, and in turn, improve the material removal rate and spark gap.
2. The EWR drops significantly with the increase of carbon nanofiber concentration, especially under the time-controlling conditions.
3. Increasing carbon nanofiber concentration is helpful to prevent tool tip concavity formation, and in turn, improves form accuracy of micro cavity.
4. Without carbon nanofiber addition, the RB-SiC material was removed by spalling of large flakes, causing large surface craters. With fiber addition, however, the crater size could be dramatically reduced.
5. Surface finish can be improved by adding carbon nanofibers in the dielectric fluid. The lowest surface roughness was achieved at a fiber concentration of 0.02–0.1 g/L.
6. The mechanism of micropore formation on RB-SiC at high carbon nanofiber concentration involves preferential removal of silicon binder, apart from the ejection of gases in EDM of metal materials.
7. Carbon nanofibers were partially adhered to the workpiece surface, especially when a high concentration of carbon nanofibers was used.
8. There is a bidirectional material migration between the electrode and the workpiece surface. Adding carbon nanofibers in the dielectric fluid at a suitable concentration is helpful for preventing the material migration.

References

Chow, H.M., Yang, L.D., Lin, C.T., Chen, Y.F., 2008. The use of SiC powder in water as dielectric for micro-slit EDM machining. Journal of Materials Processing Technology 195, 160–170.

Clijsters, S., Liu, K., Reynaerts, D., Lauwers, B., 2010. EDM technology and strategy development for the manufacturing of complex parts in SiSiC. Journal of Materials Processing Technology 210, 631–641.

Ekmekci, B., Sayar, A., 2013. Debris and consequences in micro electric discharge machining of micro holes. International Journal of Machine Tools and Manufacture 65, 58–67.

Ekmekci, B., Sayar, A., Opoz, T.T., Erden, A., 2009. Geometry and surface damage in micro electrical discharge machining of micro-holes. Journal of Micromechanics and Microengineering 19, 105030.

Ekmekci, B., Ersoz, Y., 2012. How suspended particles affect surface morphology in powder mixed electrical discharge machining (PMEDM). Metallurgical and Materials Transactions B 43B, 1138–1148.

Gunawan, S.P., Mahardika, M., Hamdi, M., Wong, Y.S., Mitsui, K., 2009. Effect of micro-powder suspension and ultrasonic vibration of dielectric fluid in micro-EDM processes – Taguchi approach. International Journal of Machine Tools and Manufacture 49, 1035–1041.

Gunawan, S.P., Muslim, M., Hamdi, M., Wong, Y.S., Mitsui, K., 2011. Accuracy improvement in nanographite powder suspended dielectric fluid for micro electrical discharge machining processes. The International Journal of Advanced Manufacturing Technology 56, 143–149.

Jahan, M., Rahman, M., Wong, Y., 2010a. Modelling and experimental investigation on the effect of nanopowder mixed dielectric in micro electrodischarge machining of tungsten carbide. Proceedings of the Institution of Mechanical Engineers, Part B: Journal Engineering Manufacture 224 (11), 1725–1739.

Jahan, M., Rahman, M., Wong, Y., 2010b. Study on the nano-powder-mixed sinking and milling micro-EDM of WC–Co. The International Journal of Advanced Manufacturing Technology 53, 167–180.

Klocke, F., Zunke, R., 2009. Removal mechanisms in polishing of silicon based advanced ceramics. Annals of the CIRP 58 (1), 491–494.

Konig, W., Dauw, D., Levy, G., Panten, U., 1998. EDM-future steps towards the machining of ceramics. Annals of the CIRP 37 (2), 623–631.

Lauwers, B., Kruth, J.P., Liu, W., Eeraerts, W., Schacht, B., Bleys, P., 2004. Investigation of material removal mechanism in EDM of composite ceramic materials. Journal of Materials Processing Technology 149, 347–352.

Lee, L.C., Lim, L.C., Narayanan, V., Venkatesh, V.C., 1988. Quantification of surface damage of tool steels after EDM. International Journal of Machine Tools and Manufacture 28 (4), 359–372.

Paramjit, S., Anil, K., Naveen, B., Vijay, K., 2010. Some experimental investigation on aluminium powder mixed EDM on machining performance of hastelloy steel. International Journal of Advanced Engineering Technology 1/2, 28–45.

Puertas, I., Luis, C.J., 2004. A study on the electrical discharge machining of conductive ceramics. Journal of Materials Processing Technology 153/154, 1033–1038.

Soni, J.S., Chakraverti, G., 1996. Experimental investigation on migration of material during EDM of die steel (T215 Cr12). Journal of Materials Processing Technology 56, 439–451.

Suyama, S., Kameda, T., Itoh, Y., 2003. Development of high-strength reaction-sintered silicon carbide. Diamond and Related Materials 12, 1201–1204.

Takashi, E., Takayuki, T., Kimiyuki, M., 2008. Study of vibration assisted micro EDM – the effect of vibration on machining time and stability of discharge. Precision Engineering 32, 269–277.

Tani, T., Fukuzawa, Y., Nambu, K., Mori, N., 2002. Machining phenomena in EDM of insulating ceramics with powder mixed oil. Journal of the Japan Society of Electrical Machining Engineers 36 (81), 39–46.

Tam, H.Y., Cheng, H.B., Wang, Y.W., 2007. Removal rate and surface roughness in the lapping and polishing of RB-SiC optical components. Journal of Materials Processing Technology 192/193, 276–280.

Trueman, C.S., Huddleston, J., 2000. Material removal by spalling during EDM of ceramics. Journal of European Ceramic Society 20, 1629–1635.

Tzeng, Y.F., Chen, F.C., 2005. Investigation into some surface characteristics of electrical discharge machined SKD-11 using powder-suspension dielectric oil. Journal of Materials Processing Technology 170, 385–391.

Wilhelm, M., Kornfeld, M., Wruss, W., 1999. Development of SiC–Si composites with fine-grained SiC microstructures. Journal of the European Ceramic Society 19, 2155–2163.

Yan, J., Zhang, Z., Kuriyagawa, T., 2009. Mechanism for material removal in diamond turning of reaction-bonded silicon carbide. International Journal of Machine Tools and Manufacture 49, 366–374.

Yeo, S.H., Tan, P.C., Kurnia, W., 2007. Effect of powder additives suspended on dielectric on crater characteristics for micro electrical discharge machining. Journal of Micromechanics and Microengineering 17, 91–98.